Silicon energetic dust particles as carbon-free energy carriers

H. Heng*, C. Mani, N. Chepel, K. Mangalvedhe, E. Antar, S. Goroshin, J. Bergthorson
McGill University
Department of Mechanical Engineering, McGill University
817 Sherbrooke Street West, Montreal, Quebec, H3A 0C3, Canada

1 Introduction

Metal fuels, including silicon, are receiving significant attention as zero-carbon energy carriers. Silicon is an especially appealing energy carrier for terrestrial use due to its abundance and remarkable energy density (9 kWh/kg). Production of silicon from abundant sand sources, potentially powered by solar energy in desert regions, provides a pathway for carbon-neutral silicon smelting [1]. Advanced methods for producing silicon, such as molten salt electrolysis or solar furnace technology, can facilitate its reduction from SiO_2. Given the abundant sand resources in deserts, sustainability concerns related to sand extraction are unlikely to arise. Thus, the burnt silicon dioxide can either be repurposed locally for cement or ceramic production, which also eliminates the energy consumption for transporting the burnt silicon dioxide for reduction. Silicon's potential extends to space applications as silicon dioxide (SiO_2) is the single most abundant element both in lunar regolith and Martian soil. Locally produced silicon and oxygen can be used as propellant for rocket propulsion systems.

Despite its high potential and favourable properties, silicon is rarely considered as a fuel, making its combustion data limited. This is largely due to the fact that silicon is relatively difficult to ignite and self-sustain in vigorous combustion compared to other conventional fuels. Existing studies on silicon combustion primarily focus on its role in pyrotechnics or as a component in metalloid-based composite solid propellants. In this work, premixed silicon Bunsen flames were successfully stabilized for the first time using a self-developed Bunsen dust burner. This breakthrough enabled a systematic investigation of silicon's combustion behaviour, including burning velocity, combustion temperature, and analysis of condensed combustion products — research areas in silicon combustion where data are currently scarce or unavailable in the literature. These findings offer valuable insight into the combustion mode of silicon, affirm its feasibility as a fuel, and establish a foundational basis for future industrial safety assessments, practical applications, and engineering designs related to silicon combustion.

2 Experimental Setup

The silicon powder used in the experiment is supplied by EdgeTech Industries LLC with 99.9% purity. The particles are irregularly shaped, with a mean Sauter diameter of d_{32}= 2.33 μm. In the present work, the silicon particles are oxidized with two different gas mixtures, composed of 30%O_2 and 40%O_2 by mole, with nitrogen gas used as the diluting gas.

* Correspondence to: cloud.heng@mail.mcgill.ca

A new dust burner setup was developed and constructed, building on prior experimental work experience, with enhanced features designed to stabilize the combustion of slower-burning metal fuels. The schematic of the dust burner is provided in Fig. 1. In this setup, silicon particles are pre-loaded into a powder reservoir. The powder in the reservoir is driven by a linear actuator and dispersed with an oxidizing gas through a concentric air-knife system similar to the design detailed in [2]. Once dispersed, the silicon-nitrogen-oxygen suspension flows through a 60-cm long laminarizing tube. To regulate the flow rate in the laminarizing tube after dispersion, pure nitrogen gas is injected into a calibrated ejector system, creating a venturi effect to bypass a portion of the flow in the laminarizing tube. A propane-oxygen gas mixture is supplied to the nozzle, forming a tiny ring pilot flame around the nozzle exit (see component 5 in Fig. 1), serving as a flame holder and aiding in flame stabilization.

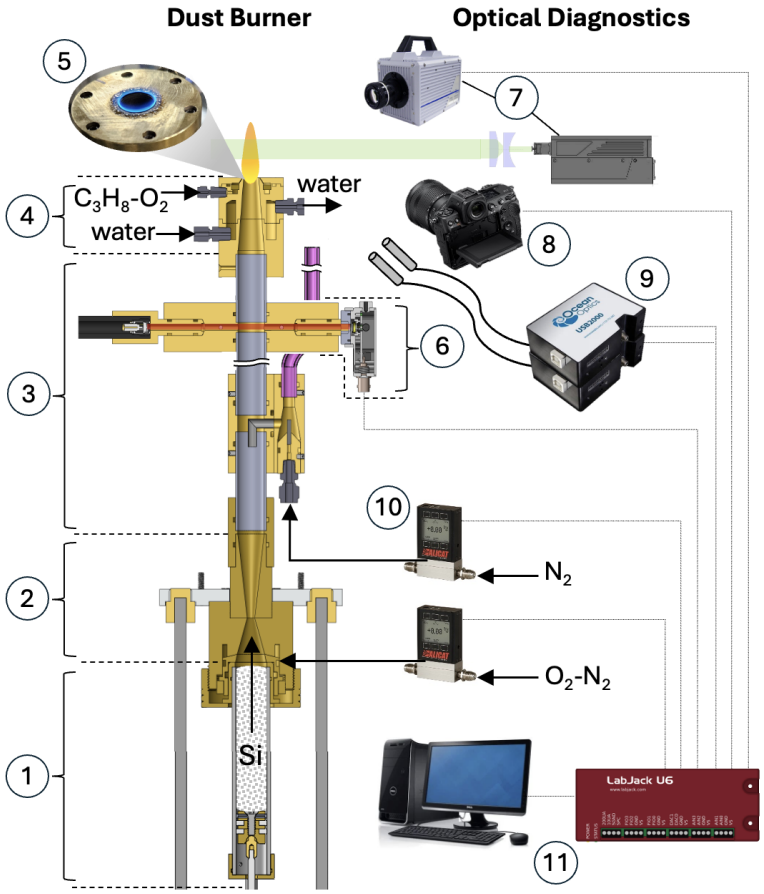

Figure 1: [Left side] Dust burner setup design: (1) silicon powder reservoir driven by a linear actuator, (2) dispersion system with a concentric air-knife flow and converging-diverging section, (3) 60-cm long laminarizing tube with an ejector system to divert the flow to a bypass tube, (4) conical nozzle system with (5) a water-cooled ring flame holder with a tiny circular propane-oxygen pilot flame. [Right side] Optical diagnostic tools: (6) laser attenuation system for particle concentration monitoring with a 5 mW red laser and a photodiode, (7) PIV system with a 5 W green laser and a high-speed camera, (8) digital mirrorless camera, (9) spectrometers with 200-1100 nm and 260-400 nm range connected to fiber optic cables, (10) gas flow meters, (11) data acquisition system.

A new dust concentration monitoring system is designed, allowing direct measurement within the laminarizing tube by analyzing the attenuation of a 5 mW red laser beam passing across the tube's diameter with a photodiode. This laser probe is calibrated according to the Beer-Lambert law, where a linear relationship between the laser beam attenuation and the particle concentration is established.

A Nikon Z8 digital camera captures the flame contours of the stabilized silicon flames, which are then used to estimate the flame surface area. The burning velocity, S_L is calculated by dividing the volumetric flow rate, $\dot{V}$ at the nozzle exit by the estimated flame surface area, A_f: $S_L = \dot{V}/A_f$. As a complementary verification method, the Particle Image Velocimetry (PIV) technique is performed. A 5 W green laser (532 nm wavelength) is utilized to form a 1 mm x 15 mm laser sheet that illuminates the particles in stabilized silicon flames at about 15-30 mm above the nozzle exit. The motion of these illuminated particles is recorded by a Photron SA5 high-speed camera.

To estimate the combustion temperature, a calibrated Ocean Optics HR4000 spectrometer is used to capture the continuous emission spectra of the condensed products in the stabilized flames across a wavelength range of 200-1100 nm. Another calibrated HR4 Pro spectrometer with a higher resolution in the 260-400 nm range is used to observe excited SiO emissions. Each spectrometer is connected via a fiber optic cable to collect light from the stabilized flames. Data from all the optical devices, along with inputs from all the mass flow meters, are synchronized in a data acquisition system.

3 Experimental Results

Bunsen-type silicon dust flames are successfully stabilized in two oxidizing mixtures: 30%O_2-70%N_2 and 40%O_2-60%N_2. The typical images of silicon Bunsen flames stabilized in dust flow at a wide range of fuel concentrations and two different oxygen concentrations are shown in Fig. 2.

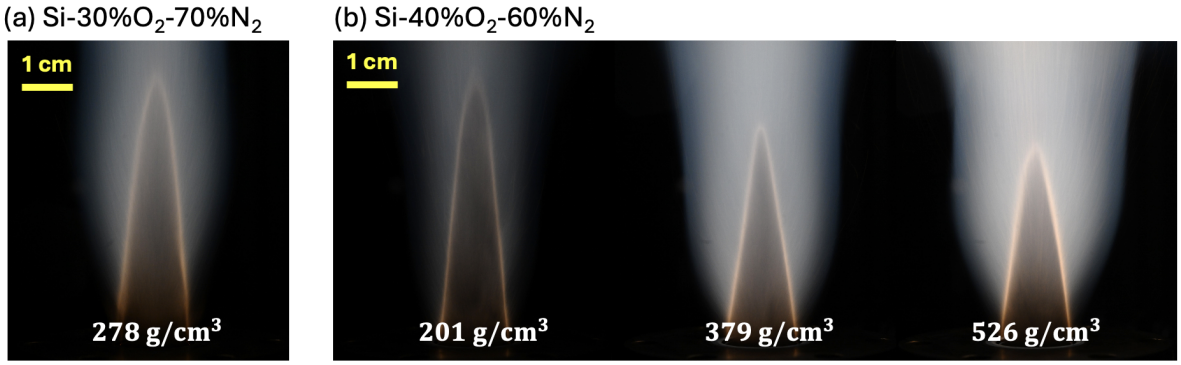

Figure 2: Stabilized silicon flames on the dust burner taken with the same camera exposure settings: (a) Si-30%O_2-70%N_2 suspension (b) three sample frames for Si-40%O_2-60%N_2 suspension at different particle concentrations, with the same volumetric flow rate at the nozzle exit

The burning velocity of stabilized silicon flames measured in this study is shown in Fig. 3. The burning velocity, derived using the flame contour method, is found to be comparable to that measured using the PIV method for both oxidizing gas environments. However, PIV measurements exhibit high uncertainties due to the need for a high particle seeding density to stabilize the flame. This leads to attenuation of the laser beam caused by light scattering from silicon particles and nano-sized combustion product particles. As the silicon particle concentration increases, the available surface area for the combustion reaction also increases, resulting in a steady increase in the burning velocity. A noticeable increase in burning velocity is also observed when the oxygen concentration rises from 30% to 40% due to a higher oxygen diffusion rate. Figure 3 also compares the silicon burning velocities obtained in this study with those of other metal fuels reported in two previous studies [3,4], which used the PIV method to examine the burning velocities of aluminum and iron flames, respectively, at various O_2 concentrations diluted with nitrogen in a similar Bunsen dust flame configuration. The burning velocity of silicon appears to be comparable to that of aluminum-air suspension only when the silicon is burned at an elevated oxygen concentration of 40%. This suggests that, given the same particle and oxygen concentrations, the

burning velocity of silicon is slower than that of aluminum, as aluminum combustion generates a higher adiabatic flame temperature. When comparing the combustion of silicon and iron, the burning velocity of silicon appears to be similar to that of iron.

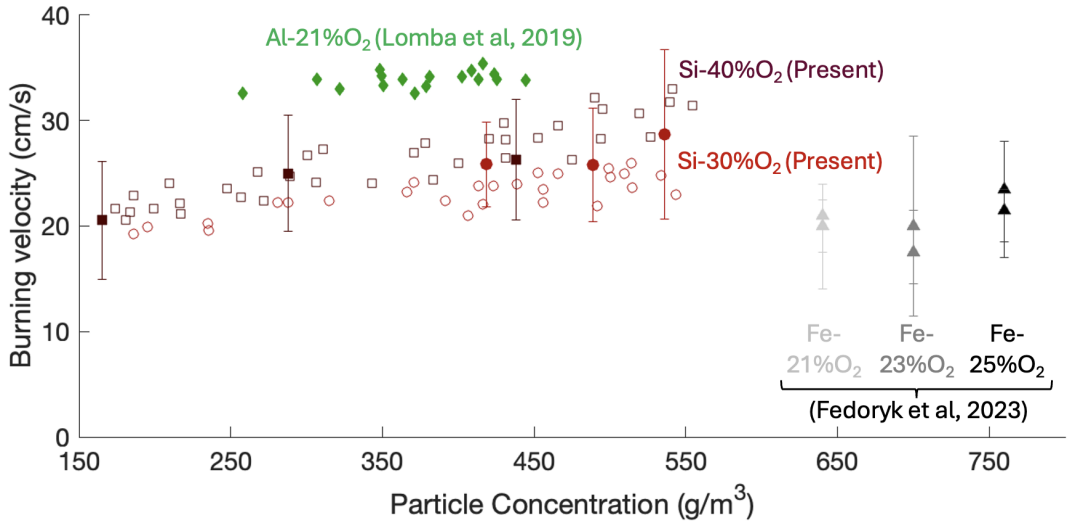

Figure 3: The burning velocity of silicon dust flame varies with particle concentrations at 30%O_2 and 40%O_2 in the present study compared to aluminium dust flame at 21%O_2 [3] and iron dust flame at 21-25%O_2 [4]. All data sets presented use nitrogen as the diluting gas. Open symbols: Measurements from the cone method ($S_L = \dot{V}/A_f$); filled symbols: Measurements from the PIV technique

The continuous emission spectra obtained from these experiments are fitted polychromatically based on Planck's law to determine the flame temperature. Figure 4 shows the resulting flame temperature, which is compared to the adiabatic flame temperature estimated using the thermodynamic equilibrium solver NASA CEARUN. In this study, a high fit quality ($R^2 = 0.999$) is achieved by applying a wavelength-dependent emissivity at $\epsilon \propto 1/\lambda^4$. The strong emissivity dependency suggests multiple scattering effects due to the formation of nano-oxide SiO_2 particles. The temperature results from these experiments align closely with the range of silicon-air maximum combustion temperatures measured by [5]. Notably, Figure 4 illustrates that the temperature data derived from both experimental data and thermodynamic equilibrium solver do not exhibit significant differences despite significant variations in both particle and oxygen concentrations. For silicon combustion, the gaseous SiO formation is expected from the thermodynamic equilibrium calculations, and it is evident from the emission spectra captured by the spectrometer in the wavelength range of 260-285 nm. This suggests that the dissociation of SiO_2 into SiO is significant in the combustion zone. As the silicon fuel concentration increases, the chemical energy available in the system rises. However, part of this energy is then stored in the form of chemical energy of SiO intermediate product instead of fully converted into heat energy in the combustion zone. Consequently, SiO formation rises with increasing particle concentration, resulting in a 'limiting temperature' for silicon combustion that is independent of both oxygen and particle concentrations.

The condensed combustion products are collected above the stabilized silicon flames in these experiments. The morphology of the reactant and the product powders are analyzed through SEM imaging, as shown in Figure 5(a) and Figure 5(b), respectively. The SEM images reveal that the condensed products are nano-oxides, with particle sizes at least one order of magnitude smaller than the initial silicon reactant particles. The combustion products are spherical, and no clustering of oxide formation is observed on the surfaces of the silicon particles. There are also no significant morphological differences noted between the two oxidizing environments. The combustion products are further analyzed using XRD, as

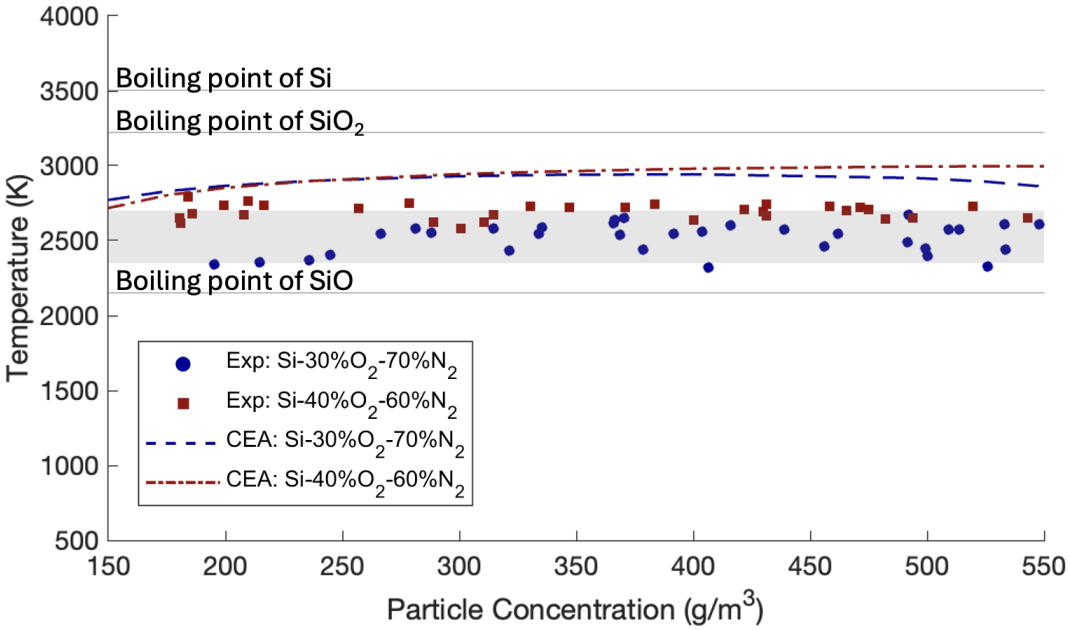

Figure 4: The estimated flame temperature of silicon dust flame varies with particle concentrations at 30%O_2 and 40%O_2 compared to the thermodynamic prediction using CEARUN and boiling point of silicon and its (sub)oxides. The shaded gray area represents the maximum temperature range measured by [5] for silicon-air flame in a Hartmann tube.

shown in Figure 5(c). The results indicate that the condensed products are amorphous in both oxidizing environments. This is due to a sharp temperature gradient between the combustion zone and the condensed silicon dioxide, significantly reducing the cooling time available for crystal structure formation.

4 Discussion: Combustion mode of silicon

Given that the boiling point of silicon is about 900 K higher than the temperatures measured in the experiments, the silicon particle is expected to burn heterogenously in the liquid phase, with the combustion reaction occurring at the particle surface in contact with oxygen molecules. This combustion mode is in consistent with the hypothesis outlined in [6] and is similar to carbon. Both silicon and carbon, with flame temperatures below their respective boiling points, underscore a shared heterogeneous combustion mode. Notably, they belong to the same group in the periodic table and have the same number of valence electrons. Like carbon, which produces CO as an intermediate that later oxidizes into CO_2, silicon combustion forms SiO, which subsequently oxidizes to SiO_2 and converts the remaining chemical energy in the intermediate SiO species to heat energy during the cooling process. However, unlike carbon, which results in gaseous CO_2, silicon's final oxidation product is condensed nano-oxide SiO_2 particles.

The stabilization of a silicon Bunsen flame on a laminar dust burner has been achieved for the first time. This breakthrough enables a detailed investigation of silicon combustion behaviours. Although the concept of utilizing silicon as a global carbon-free energy carrier has been explored in the previous literature, driven by its abundance and remarkable energy density, demonstrating the technical feasibility of silicon combustion is crucial to realizing this vision. This study addresses this challenge by showing that silicon is not only theoretically viable but also technically practical as an energy carrier, as evidenced by its ability to stabilize on a laminar dust burner, similar to aluminum and iron dust flames.

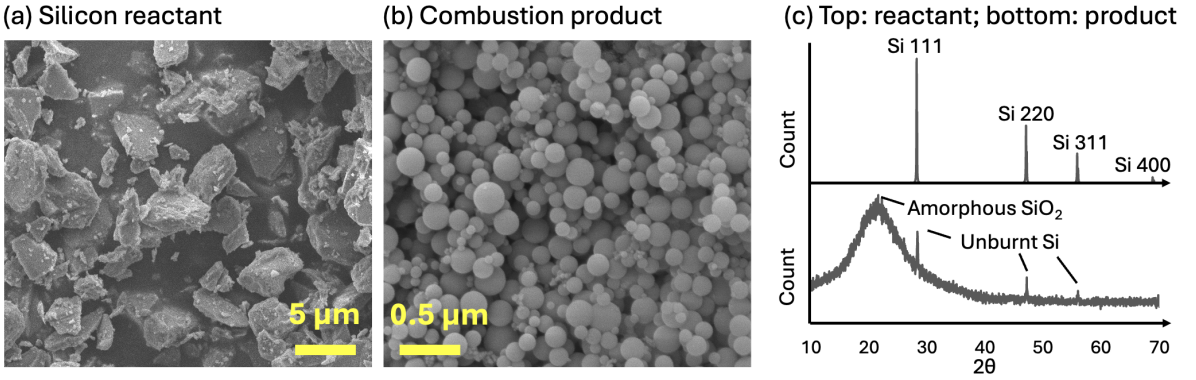

Figure 5: Comparison of the morphology for the (a) silicon reactant and (b) condensed silicon dioxide produced from the Si-30%O_2-70%N_2 flame. (c) The XRD analysis on the reactant (top) and the combustion product of the Si-30%O_2-70%N_2 flame (bottom). No significant differences are observed for two different oxidizing environments.

Acknowledgements

The project is funded by the Canadian Space Agency through the Flights and Fieldwork for the Advancement of Science and Technology (FAST) Grant Program (Grant No: 21FAMCGA17 and 23FAMCGA55). Student work was supported by the Natural Sciences and Engineering Research Council of Canada (NSERC), Fond de Recherche du Québec Nature et Technologies (FRQ-NT), the Schulich Foundation, and McGill University through the Vadasz Scholars. The craftsmanship of Mr. Andreas Hofmann during the fabrication process is also gratefully acknowledged.

References

[1] W. E. Bardsley, "The Sustainable Global Energy Economy: Hydrogen or Silicon?," *Natural Resources Research*, vol. 17, pp. 197–204, Dec. 2008.

[2] S. Goroshin, J. Palečka, and J. M. Bergthorson, "Some fundamental aspects of laminar flames in nonvolatile solid fuel suspensions," *Progress in Energy and Combustion Science*, vol. 91, p. 100994, July 2022.

[3] R. Lomba, P. Laboureur, C. Dumand, C. Chauveau, and F. Halter, "Determination of aluminum-air burning velocities using PIV and Laser sheet tomography," *Proceedings of the Combustion Institute*, vol. 37, no. 3, pp. 3143–3150, 2019.

[4] M. Fedoryk, B. Stelzner, S. Harth, and D. Trimis, "Laminar burning velocity measurements and stability map determination of Fe-N2/O2 mixtures in a tube burner," in *Proceedings of the European Combustion Meeting 2023*, 2023.

[5] V. Weiser, E. Roth, S. Kelzenberg, A. Raab, and O. Schulz, "Ignition and Combustion Phenomena of Silicon Particles in the Scope to Use it as a Green Fuel in Coal Power Plants," in *Proceedings of the European combustion meeting*, pp. 1–5, 2003.

[6] J. Bergthorson, S. Goroshin, M. Soo, P. Julien, J. Palecka, D. Frost, and D. Jarvis, "Direct combustion of recyclable metal fuels for zero-carbon heat and power," *Applied Energy*, vol. 160, pp. 368–382, Dec. 2015.